



Next-generation models and genetic therapies for rare neuromuscular diseases

Grant agreement No. 101080690

**D1.2 - Method to perfuse, stimulate and miniaturise 3D muscle models**

Lead partner	KCL
Other contributors	BIOND

Dissemination level	Public (PU)
Contractual date of delivery	M18, 31/11/2024
Actual date of submission	M19, 17/12/2024
Work Package	WP1
Type	Report
Version	V0.4



## Copyright

© Copyright 2024 MAGIC Consortium consisting of:

1. Institut National de la Sante et de la Recherche Medicale (INSERM), France
2. Medizinische Hochschule Hannover (MHH), Germany
3. Université Paris XII Val de Marne (UPEC), France
4. Children’s Hospital Medical Center (CCHMC), USA
5. National University of Ireland Maynooth (NUIM), Ireland
6. Parent Project aps (PP), Italy
7. BI/OND Solutions BV (BIOND), Netherlands
8. Stichting Duchenne Data Foundation (DDF), Netherlands
9. VIVEbiotech sl (VIVE), Spain
10. ReiThera srl (RT), Italy
11. Siegfried DiNAMIQS (DNMQS), Switzerland
12. The Francis Crick Institute Limited (CRICK), UK
13. King’s College London (KCL), UK
14. Muscular Dystrophy Group of Great Britain and Northern Ireland (MDUK), UK
15. University College London (UCL), UK
16. Gulbenkian Institute For Molecular Medicine (GIMM), PT

This document may not be copied, reproduced, or modified in whole or in part for any purpose without written permission from the MAGIC Consortium. In addition to such written permission to copy, reproduce, or modify this document in whole or part, an acknowledgement of the authors of the document and all applicable portions of the copyright notice must be clearly referenced. All rights reserved.

## Disclaimer

The content of this deliverable does not reflect the official opinion of the European Union. Responsibility for the information and views expressed herein lies entirely with the author(s).



## History

Version	Date	Description	Reviewer
V0.1	25/11/2024	Addition of BIOND section for internal review	NG & MH
V0.2	06/12/2024	Addition of KCL with BIOND section for internal review	AS & EC
V0.3	10/12/2024	KCL & BIOND section for internal review	SD
V0.4	16-17/12/2024	Final revision and Submission to EU	

## Authors list

Organisation	Name	Email
KCL	Andrea SERIO (AS)	andrea.serio@kcl.ac.uk
KCL	Eugenia CARRARO (EC)	eugenia.carraro@kcl.ac.uk
BIOND	Nikolas GAIO (NG)	nikolas@biondteam.com
BIOND	Mitchell HAN (MH)	m.han@biondteam.com
UCL	Francesco Saverio TEDESCO (FST)	f.s.tedesco@ucl.ac.uk
UCL	Sumitava DASTIDAR (SD)	s.dastidar@ucl.ac.uk

## Table of Contents

Executive Summary .....	7
Materials and Methods .....	7
Protocol of muscles generation on MUSbit™ chip .....	9
Developed technology .....	9
Summary of activities and research findings .....	15
1. Miniaturization of 3D muscle generation devices .....	15
2. Stimulation of miniaturized 3D muscle .....	21
3. Perfusion of our 3D muscle generation devices .....	24
Conclusions.....	31

## List of Figures

Figure 1 Rendering of the MUSbit™ chip .....	8
Figure 2 Picture of the comPLATE™interface, equipped with 6MUSbit™ chips .....	9
Figure 3 Stimulation device and accessories. ....	10
Figure 4 Screenshot of the software developed to control the stimulation device. ....	11
Figure 5 Pneumatic device component description. ....	12
Figure 6 Pump cartridge LED status indicator. ....	13
Figure 7 Graphic interface of the software. ....	13
Figure 8 LEFT: an overview of the comPLATE™components, with a highlighted lid. CENTER: a rendering of the newly designed lid compatible with electrodes. RIGHT: a picture of the new prototype.....	14
Figure 9 System overview.....	14
Figure 10 Overview of the different application of our bioengineering microfabrication pipeline adapted from Hagemann, Bailey, et. al.....	15
Figure 11 Miniaturized 3D skeletal muscle generation pipeline.....	16
Figure 12 Representative images of positive and negative moulds and the final PDMS support. ....	16
Figure 13 Technical validation of the PDMS supports.....	17
Figure 14 Representative images of our casting system and the final 3D skeletal muscle product. ....	17
Figure 15 Biological validation of miniaturized 3D skeletal muscle using our PDMS supports. ....	18
Figure 16 Validation of long-lasting 3D skeletal muscle in vitro culture. ....	19
Figure 17 In vitro generation of 3D neuromuscular constructs adapting our PDMS supports.....	20
Figure 18 Calcium transients in 3D miniaturized skeletal muscle and 3D neuromuscular constructs. ....	20
Figure 19 Electrical stimulation and measurement of contraction for WT and DMD iPSC-based muscle microtissues.(A) Measurement of contraction with increasing pulse frequency. (B) Representative traces of WT and DMD microtissues stimulated with twitch or tetanic pulses at Day 14.(C) Average contraction amplitude±95%CI of sustained contraction at Day 14 (top), and boxplots of peak contraction amplitudes at Day 7, 10 and 14 (bottom). ....	22
Figure 20 The prototype of the electromagnet platform.....	23
Figure 21 The electromagnet platform, with all its components.....	23



Figure 22 Elongation and contraction of the magnetic pillar using standard and reverse polarity. .... 24

Figure 23 Straight channel negative mould design and respective PDMS support. .... 24

Figure 24 3D skeletal muscle differentiation in straight channel PDMS support with respective calcium transients. .... 25

Figure 25 Left - Microscope setup with the comPLATE; Right - comPLATE™ cross section with MUSbit™ ..... 26

Figure 26 Left – Run-in Setup; Right – Flush-out Setup ..... 26

Figure 27 Measuring the detectable volume within the setup ..... 27

Figure 28 Calibration Curve for different concentration of dye in the well (NOTE- concentration measured over a volume of 200µl) ..... 27

Figure 29 Dilution tests ..... 28

Figure 30 Measured intensity at different molar masses of the dye ..... 28

Figure 31 Run in dye Summary [C<sub>m</sub>- measured concentration] ..... 28

Figure 32 Flush out Dye summary [C<sub>m</sub> – measured Concentration] ..... 29

Figure 33 C2C12 muscle microtissue under a constant 30 µl/min flowrate for 23 hours ..... 30

Figure 34 Muscle contraction under simultaneous 1 Hz electrical pacing and 30 µl/min perfusion ..... 30



## Abbreviations and Acronyms

<b>Acronym</b>	<b>Description</b>
MAGIC	Next-Generation Models And Genetic Therapies for Rare Neuromuscular Diseases
WP	Work-Package
CAD	Computer-Aided Design
SLA	Stereolithography
PDMS	Polydimethylsiloxane
AAV	Adeno associated virus
DMD	Duchenne muscular dystrophy
FITC	Fluorescein Isothiocyanate
BDM	2,3-Butanedione monoxime

## Executive Summary

Neuromuscular diseases are a major cause of disability worldwide, characterized by muscle wasting and weakness. While gene therapy shows potential as a treatment, its development requires next generation humanized complex disease models reflective of in vivo disease physiology in humans. Hence, MAGIC's overarching goal is to develop advanced "quasi-vivo" models of human muscle disorders to serve as platforms for creating and evaluating innovative therapeutic strategies and vectors. Under WP1, we are building new robust in vitro models of human muscle and neuromuscular disorders. Previously under D1.1, we have demonstrated successfully generation of multilineage 3D muscle models using available PDMS scaffolds. Myogenic, vascular, neural and fibrogenic cells were co-cultured in different combinations relevant to the target diseases of our project, namely DMD, L-CMD, UCMD and XLCNM.

In this deliverable D1.2, we present the work undertaken to develop next generation miniaturized neuromuscular bioengineered 3D models for perfusion and stimulation. In this deliverable report, we present the technology platforms from two MAGIC partners (KCL & Bi/ond) and protocols we have optimised to both miniaturise the muscle constructs we produce, introduce different functionalities within the culture devices (e.g. perfusion, stimulation), and to characterise the physiological and cellular properties of the generated muscle tissue. As part of this deliverable, we have also optimised the coculture protocols to generate functional neuromuscular circuitry within the engineered devices. Using the enhanced platform, we characterized the model with the stimulation tool by monitoring its contraction forces, comparing healthy tissue to DMD-affected tissue. Furthermore, we investigated the impact of flow on skeletal muscle tissue and demonstrated the system's ability to dynamically administer drugs and analyse their effects on the tissue. Finally, we highlighted the intrinsic miniaturization capabilities of our system, as previously introduced in Deliverable 1.1.

## Materials and Methods

### MUSbit™ CHIP

The MUSbit™ (Figure 1) is a silicon-based microfluidic chip including micro-pillars that allow for the precise control and induction of skeletal muscle organoid formation. This feature is crucial for the accurate replication of the complex and dynamic nature of muscle tissue. Secondly, the device incorporates microfluidic channels, which enable the dynamic application of drugs within the model. This feature also allows for the performance of physiologically relevant absorption studies that can provide valuable insights into drug efficacy and side effects.

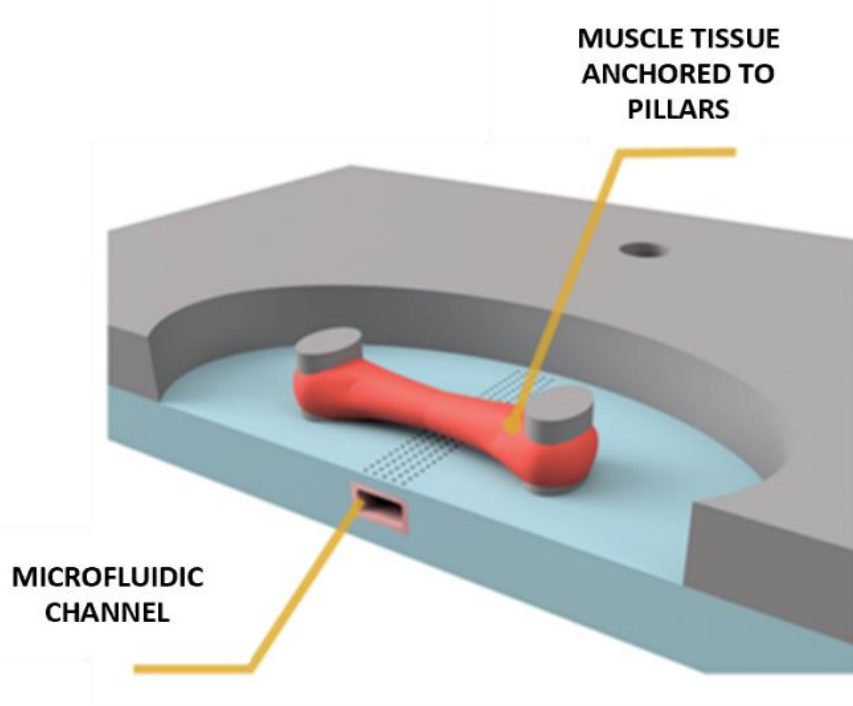


Figure 1 Rendering of the MUSbit™ chip

These silicon based chips are scalable and have the potential to integrate multiple features according to customer needs. For instance, the chips allows multiple co-cultures, muscle microenvironments with specific cells, vascularization, chronic stimulation over hours/days, contraction forces, and compatible with a diverse range of imaging techniques and conventional assays.

### **ComPLATE™**

The comPLATE™ (Figure 2) is an interface previously developed by Bi/ond for various chips and applications. This interface can accommodate up to six MUSbit™ chips and is fully compatible with pneumatic systems utilizing any type of pump. The comPLATE™ is designed to be reusable, offering versatility and cost-efficiency.



Figure 2 Picture of the comPLATE™ interface, equipped with 6MUSbit™ chips

## Cell source

The cell source for KCL's miniaturized 3D muscles is immortalised myoblasts. For BIOND's 3D tissues, bit.bio's Opti-ox™ cells were used. Opti-ox™ cells are designed to facilitate precise control over the expression of transcription factors. This advancement enhances the reprogramming efficiency of hiPSCs, streamlining the differentiation process. Here we use their ioSkeletal Myocytes™, specifically developed for rapid myogenic differentiation.

## Protocol of muscles generation on MUSbit™ chip

This deliverable builds upon the detailed protocol presented in Deliverable 1.1 for developing a DMD model using the MUSbit™ chip. Key steps include plasma treatment to render the chip hydrophilic, sterilization with ethanol or IPA, and careful preparation of the chip wells. Cells embedded in hydrogel are seeded into the chips, where they self-compact around pillars to form skeletal muscle bundles. Optimal cell densities and medium exchange protocols, tailored to specific cell types like ioSkeletal Myocytes, ensure successful bundle formation and differentiation.

## Developed technology

At the start of the project, we lacked a complete system enabling biologists to create skeletal muscle tissues, like those described in Deliverable 1.1, while also providing simultaneous stimulation and perfusion capabilities. To address this, we initially focused on designing two key modules for the platform: a stimulation tool for electrically stimulating the tissue and a pneumatic device for delivering

perfusion through the microfluidic channel. Over the past year, the Bi/ond team has successfully designed, prototyped, and conducted alpha and beta testing for these components, as detailed below.

**Stimulation tool:** The device is comprised of the stimulation component, the electrodes used for the connection with the sample tissue and a power supply. The stimulation system is the white box in the Figure 3, and it has two LEDs in the front as Status and Signal and one at the side of the power connector. The device is powered by a 5 V power supply, when the power is connected, the power LED will turn Green.

The main electrodes are connected using a BNC connector at the lower part of the device. The electrodes are then connected to the plate as needed. Once in operation, and the stimulation signal is defined over a browser interface that can be accessed when connected to the device.

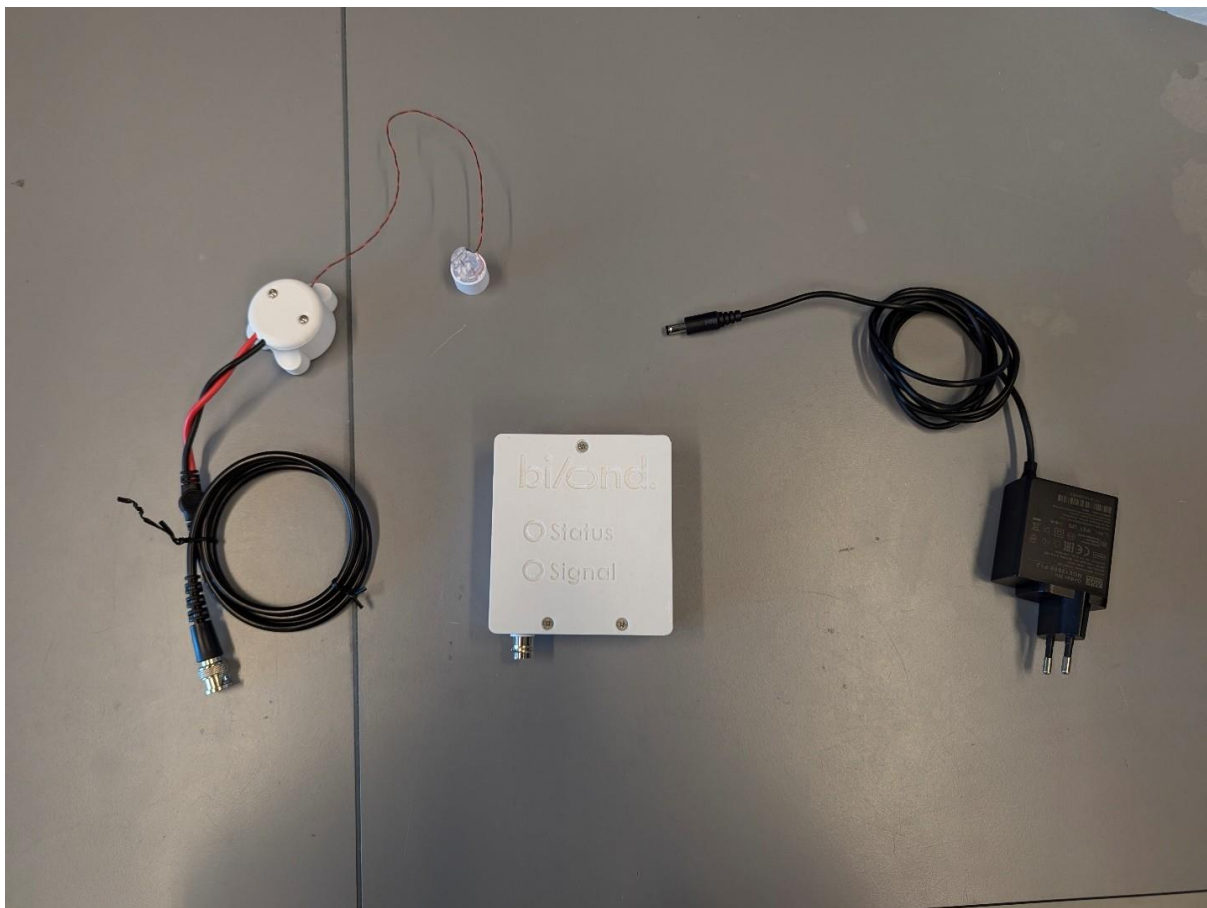


Figure 3 Stimulation device and accessories.

In conjunction with the stimulation tool, proprietary software was developed to allow users to control key stimulation parameters, such as voltage, pulse width, frequency, and pulse train duration (Figure 4).

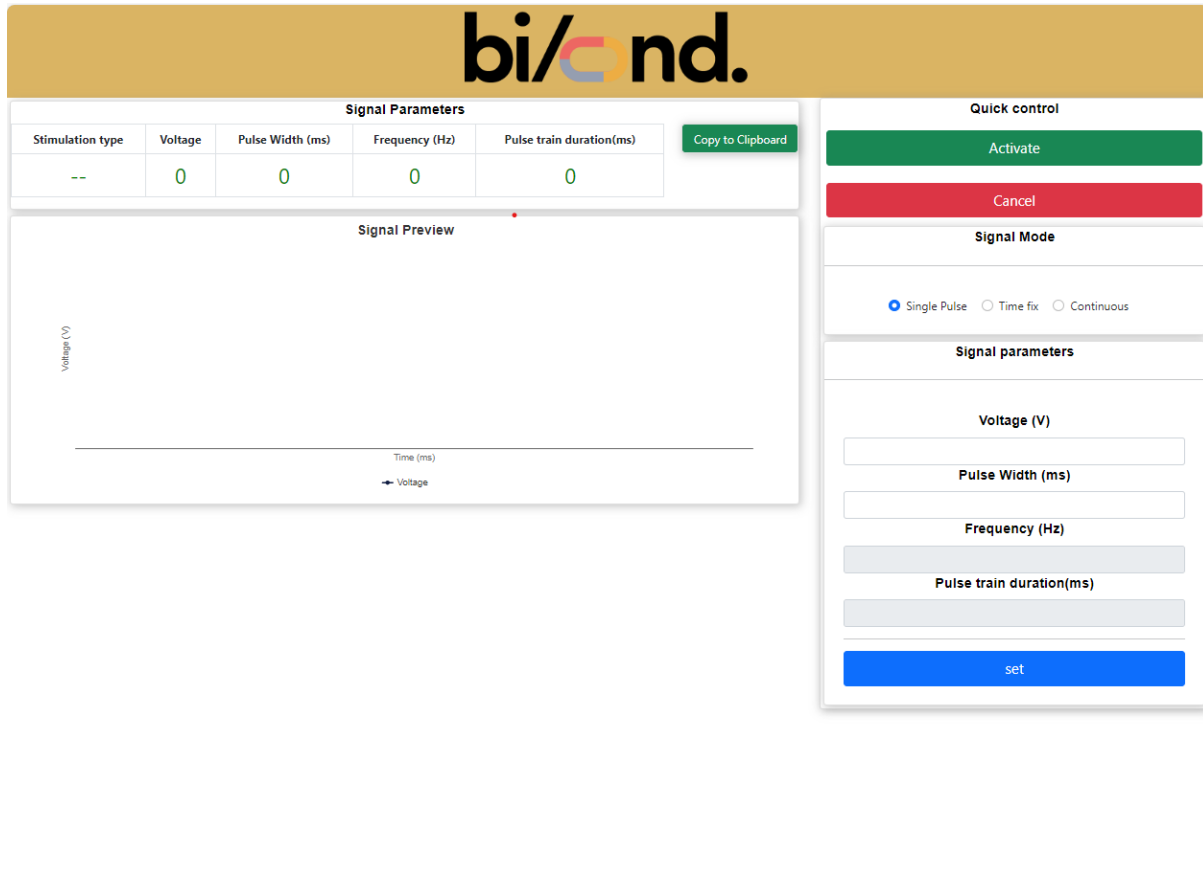


Figure 4 Screenshot of the software developed to control the stimulation device.

**Pneumatic device:** The Bi/ond pneumatic device (Figure 5) is a versatile tool designed to introduce unidirectional perfusion into individual microfluidic chips, featuring six independent pump circuits. Each circuit can be adjusted separately, allowing for customized flow rates for each chip. The pneumatic device supports two operational formats: a recirculation format, where liquid is continuously cycled through the chip, and an open format, where only fresh liquid is flushed through. The pneumatic device is compatible with Bi/ond's microfluidic chips, including MUSbit™ chips, enabling precise liquid circulation.

The device consists of several key components: a plate holding area, a reservoir holding area, pump cartridges, microfluidic tubing, and connections. Each of these components is described in detail here:

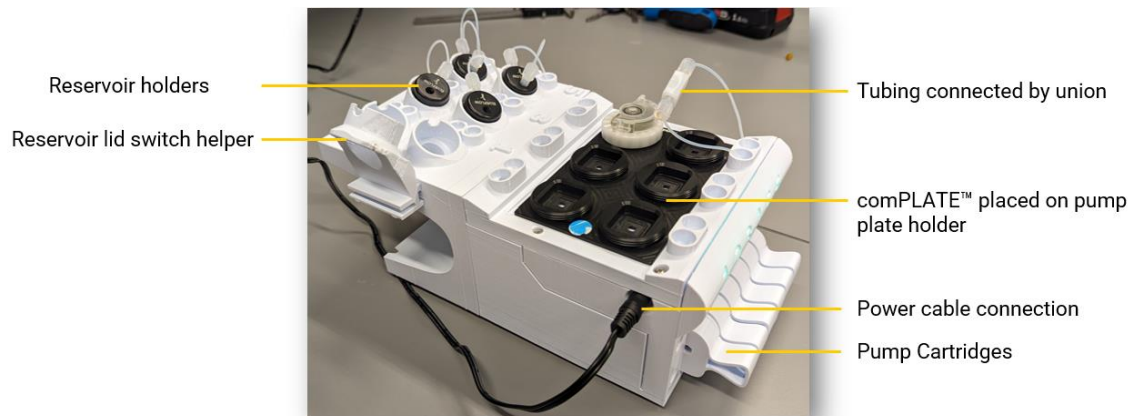


Figure 5: Pneumatic device component description.

- “Reservoir holders” hold the reservoirs attached to the pneumatic device. The reservoirs hold a maximum of 15 ml of chosen liquid to cycle through the chip. The reservoir is comprised of a lid and a standard 15 ml tube.
- The “Reservoir lid switch helper” allows for easy and sterile disassembly and assembly of the reservoir.
- The pneumatic device tubing can easily be shortened and lengthened by pulling or pushing tubing into the body of the pneumatic device. Tubings connect the reservoirs to a bridge/union or comPLATE™.
- “Pump cartridges” are individual modules attached to the pneumatic device. Pump cartridges can easily be removed and replaced by a new cartridge if necessary. The status of the cartridges is shown by a change in color in the corresponding LED as shown in Figure 6.
- The “Plate holder” is a flat area on the pneumatic device body with an indentation to allow for the comPLATE™ to fit inside without sliding off.

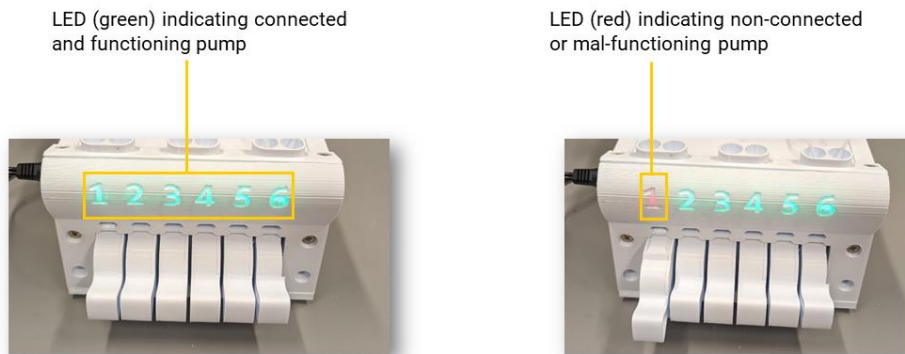


Figure 6 Pump cartridge LED status indicator.

The pneumatic device comes with its own integrated software, allowing users to set or pause flows for each individual circuit. To operate the device software, it must be plugged in and turned on.

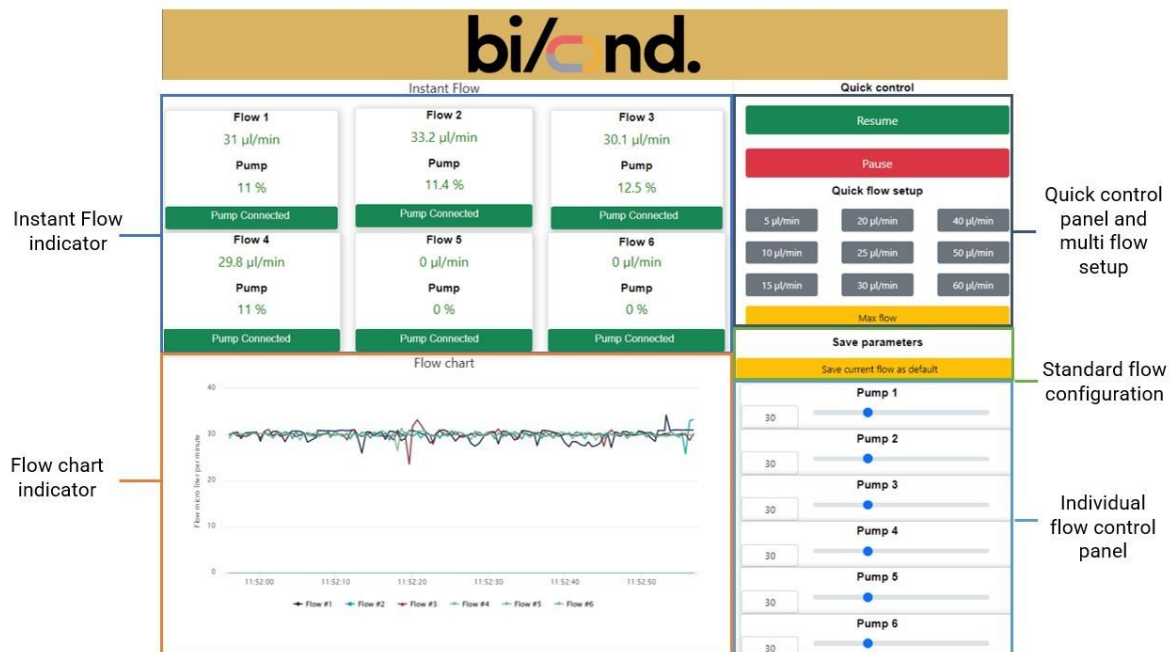


Figure 7 Graphic interface of the software.

**NEW comPLATE™ LID:** For this deliverable, the comPLATE™ was used as interface to allow biologists to interact with the MUSbiti™ chips. From a hardware perspective, to connect both stimulation tool and pneumatic devices to the

comPLATE™, we had to modify the comPLATE™ lid to accommodate the electrodes of the stimulation tool while ensuring the integrity of the comPLATE™'s sealed environment – an essential feature for the perfusion in the comPLATE™.

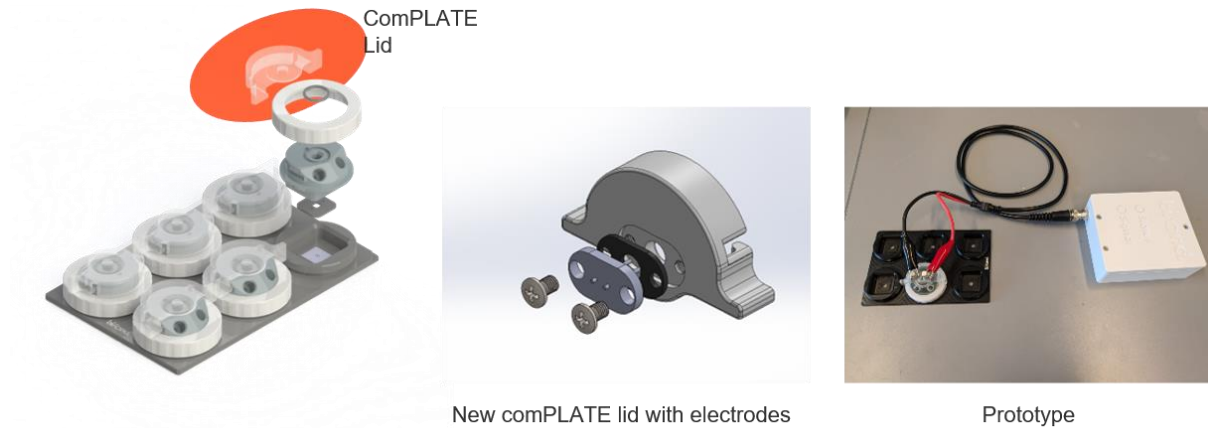


Figure 8 LEFT: an overview of the comPLATE™ components, with a highlighted lid. CENTER: a rendering of the newly designed lid compatible with electrodes. RIGHT: a picture of the new prototype.

The Bi/ond team successfully redesigned the lid, resulting in a fully integrated system that combines the miniaturized tissues presented in Deliverable 1.1 with both a stimulation device and a pneumatic tool (system overview in Figure 9).

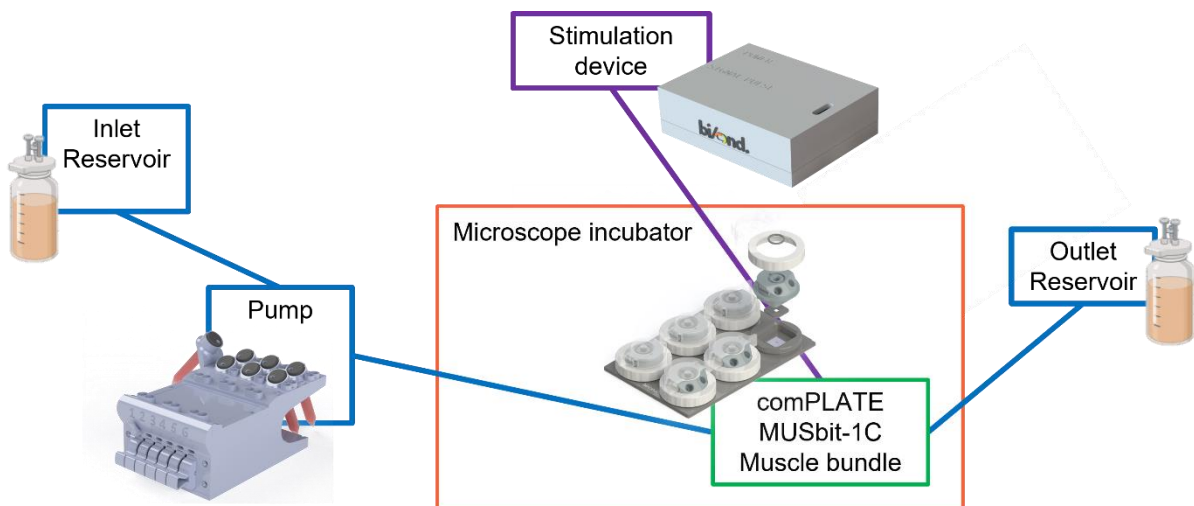


Figure 9 System overview

# Summary of activities and research findings

## 1. Miniaturization of 3D muscle generation devices

The deliverable focuses on the generation of miniaturised 3D muscle tissue with microfabricated bioengineered devices using two complementary strategies from Bi/ond and KCL.

### 1.1 Generation of miniaturized supports

Bi/ond chips are fabricated by combining conventional microfabrication techniques on silicon with scalable polymer processing. This approach ensures high reproducibility of our chips, enables the integration of electrodes and sensors, and, most importantly for this deliverable, facilitates the miniaturization of our system.

Each Bi/ond chip features a well measuring 2 x 1 mm, with pillars that are 500  $\mu\text{m}$  long and 400  $\mu\text{m}$  wide (Figure 1). These dimensions enable the creation of micro-tissues, effectively miniaturizing the 3D skeletal muscle bundles typically found in other systems. The small well volume (approximately 2  $\mu\text{L}$  for the gel and cell mixture) results in the use of a lower number of cells per well, typically ranging from 15k to 50k cells. In comparison to other systems, this represents a reduction of one, and sometimes two, orders of magnitude in cell density (e.g. A. Iuliano, *et. al.*, *Adv. Mater. Technol.* 2023).

KCL's miniaturisation approach employs an integrative approach that combines computer-aided design (CAD), stereolithography (SLA) and cell culture techniques. As recently reported in Hagemann, Bailey, *et. al.* our innovative approach can be easily adapted to study multiple biological phenomena from driven axonal elongation, to embryoid body formation and 3D skeletal muscle fabrication (Figure 10).

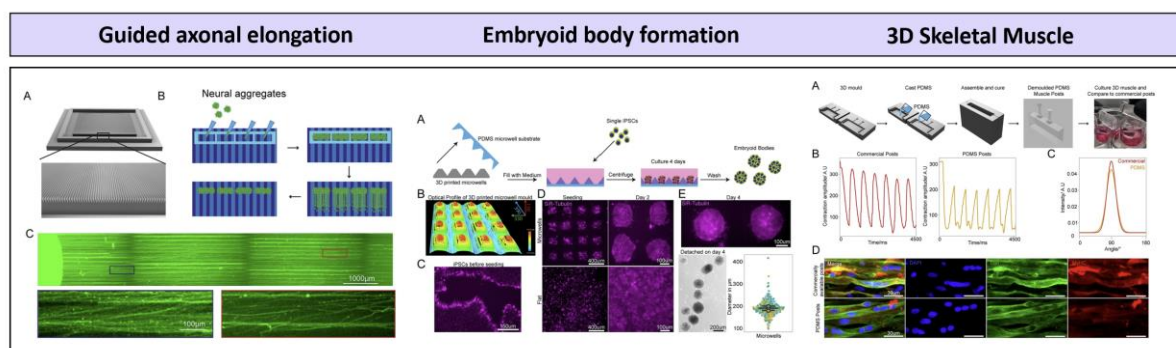


Figure 10 Overview of the different application of our bioengineering microfabrication pipeline adapted from Hagemann, Bailey, *et. al.*

Following our recent results, the fabrication of miniaturized 3D skeletal muscle is based on the development of a multi-steps pipeline (Figure 11).

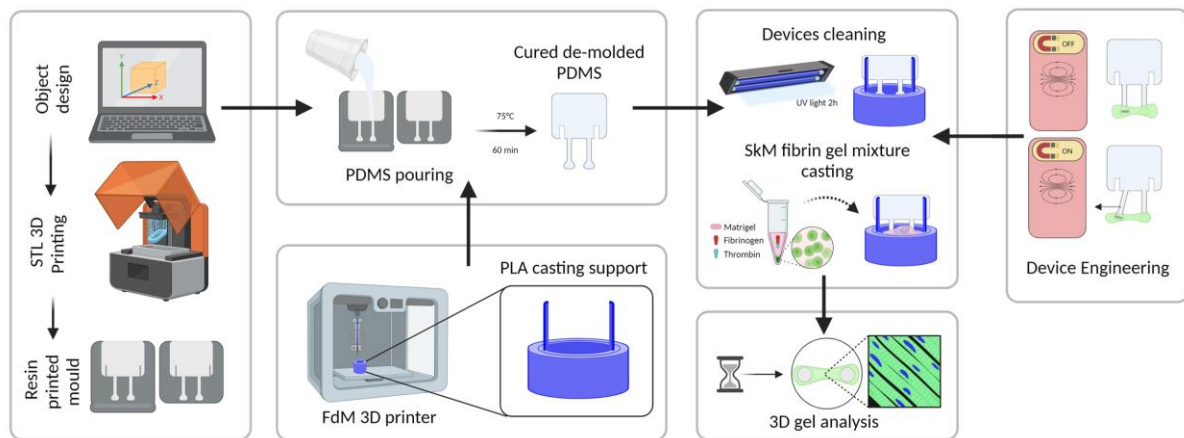


Figure 11 Miniaturized 3D skeletal muscle generation pipeline.

The skeletal muscle support design involves a dual-mould approach, comprising a positive mould for defining the 3D skeletal muscle support structure, and a negative mould to capture the inverse geometry. The negative mould is used for the actual 3D printing, leading to the generation of a resin prototype, suitable for the casting of polydimethylsiloxane (PDMS), a mouldable, biocompatible, transparent material. PDMS spontaneously cured by increasing the temperature leading to the generation of a solid and elastic support, compatible, once upon cleaning, for culturing the 3D skeletal muscles (Figure 12).



Figure 12 Representative images of positive and negative moulds and the final PDMS support.

The validation of our supports takes advantage on the use of a gel mixture composed of Matrigel, fibrin and immortalized skeletal muscle cells, but overall, the pipeline can be extended to the use of primary or hiPSCs derived myoblasts, as of other essential cell populations.

## 1.2 Validation of miniaturized supports

This miniaturization in Bi/ond's **MUSbit™ CHIP** is intrinsic to the design of their chips and was previously validated in Deliverable 1.1.

On to KCL's PDMs based 3D muscle casting platform, the pipeline was validated from both a technical and biological perspectives. One of the first key steps was assessing the accuracy of the technique, for this reason we compared the dimensions of the final PDMS supports with the ones of our CAD objects, as

expected despite the use of different geometries our constructs were able to fully recapitulate the predicted ones. In addition, we tested the versatility of our approach by generating miniaturized skeletal muscle supports with different mechanical properties, able to exert two ranges of stiffness, thus impacting on the skeletal muscle cell differentiation (Figure 13).

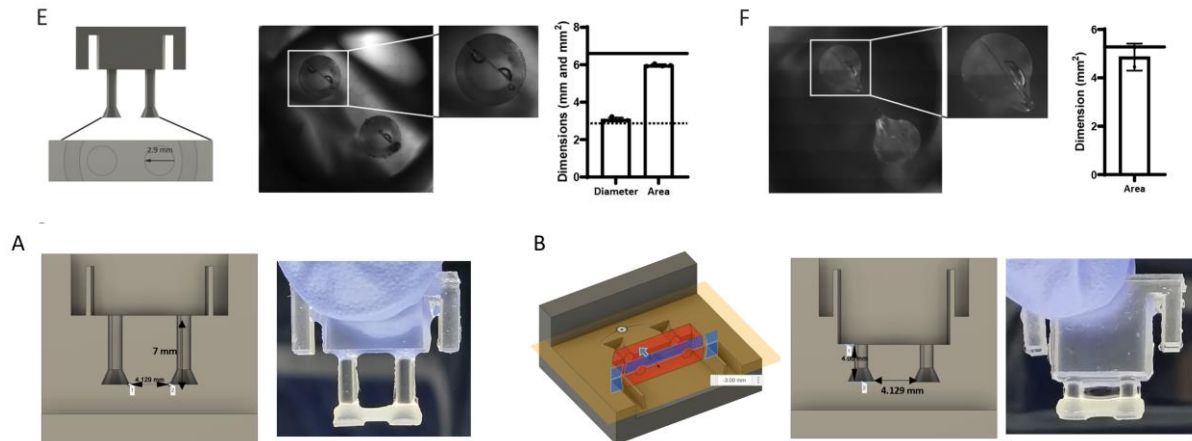


Figure 13 Technical validation of the PDMS supports.

In parallel we focused on the design and development of a novel 3D printed support for the casting of the skeletal muscle gel mixture, thus to overcome the problem of irregular skeletal muscle shapes. After multiple tests we fabricated a biocompatible casting support able to trigger the generation of homogenous longitudinal muscle (Figure 14).

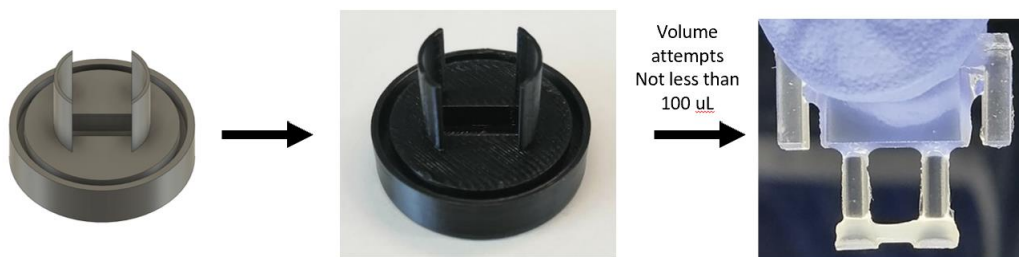


Figure 14 Representative images of our casting system and the final 3D skeletal muscle product.

From the biological perspective we believe that the generation of in vitro 3D skeletal muscle should be considered successful if the PDMS supports can sustain myoblasts differentiation and ensure homogenous and uniaxial cell orientation. For these reasons we monitored our 3D skeletal muscle over a time window of 21 days, the analysis of multiple morphometric parameters revealed the ability of our PDMS supports not only to sustain a long-lasting culture of the samples, but also an intrinsic ability to force the formation of parallel and aligned myofibers. Together with the absence of necrotic centres, as deduced by the presence of proliferative cells and uniform haematoxylin and eosin staining, we concluded

that our customized PDMS supports are a useful tool to originate healthy in vitro miniaturized 3D skeletal muscle. On the other hand, an efficient myoblasts differentiation is supported by the expression of myogenic markers, for this reason we performed immunofluorescence analysis for the detection of the mature marker TITIN. The samples imaging revealed not only a great TITIN distribution, but also the presence of skeletal muscle striations, despite the use of two different myoblasts concentration, supporting again the hypothesis that our PDMS supports can be used to generate mature in vitro miniaturized 3D skeletal muscle (Figure 15).

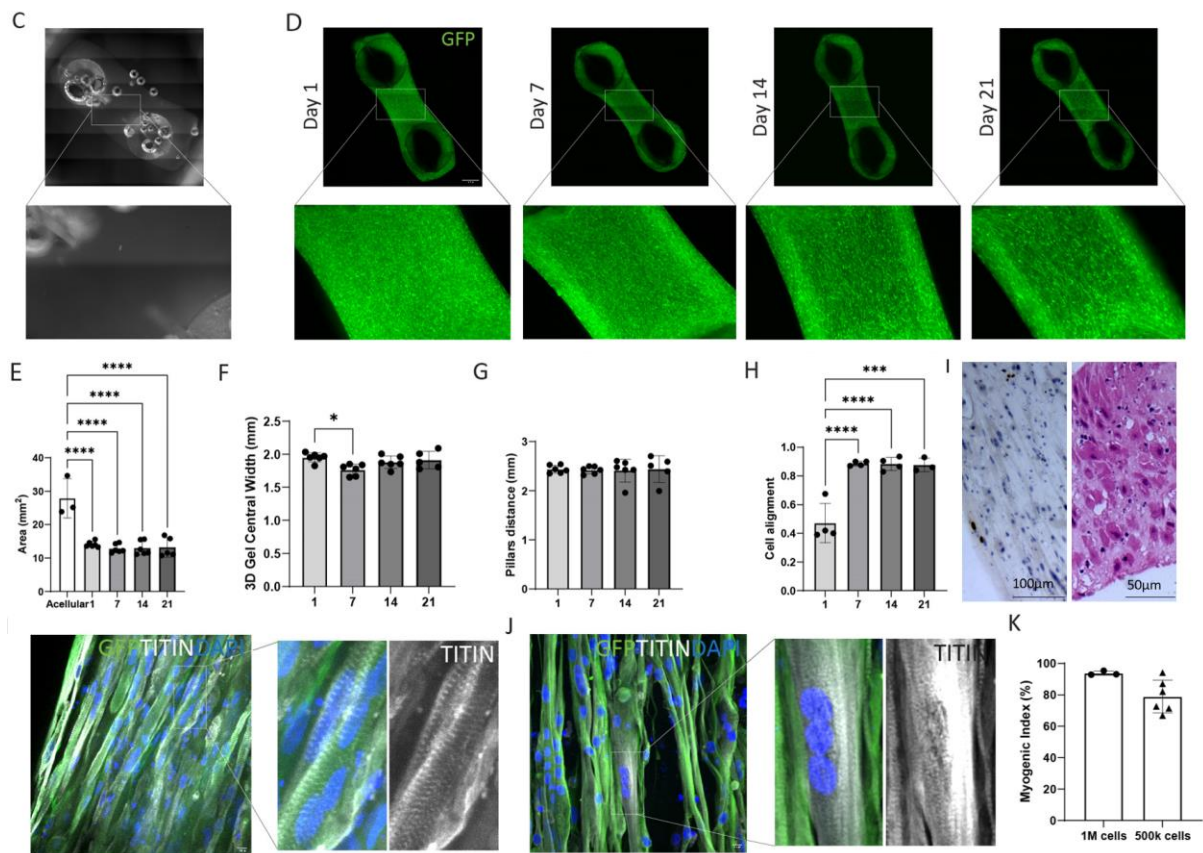


Figure 15 Biological validation of miniaturized 3D skeletal muscle using our PDMS supports.

Even though the time required for myoblasts to originate in vitro mature myofibers is cell line dependent, and should be verified for the different cell batches, we proved that our PDMS supports, when placed in the optimal cell culture conditions, can be used for other extra 7 days, for a maximum of 28 days (Figure 16), without affecting the sterility of the culture.

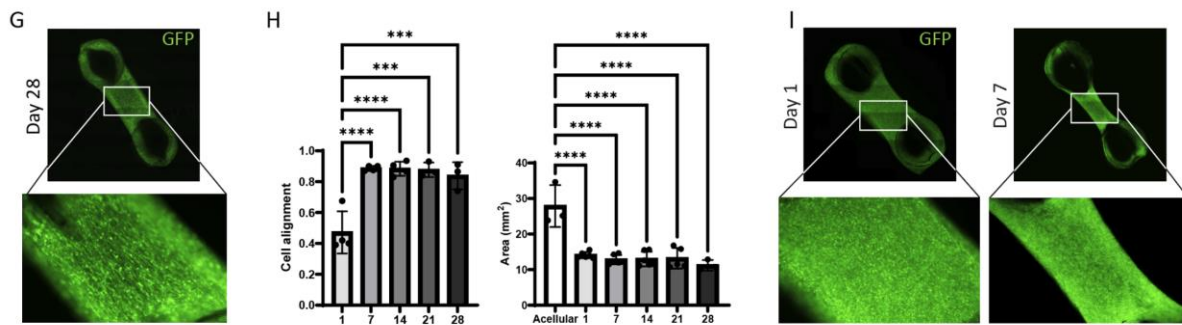


Figure 16 Validation of long-lasting 3D skeletal muscle in vitro culture.

**Generation of 3D in vitro neuromuscular constructs:** To further prove the versatility of our approach and increase the culture maturation, we adapted our PDMS supports for the addition of a second cell population. We obtained in vitro neuromuscular 3D constructs via the seeding of hiPSC derived neurospheres. When placed on the bottom of our 3D miniaturized skeletal muscles, the motor neurons contained in the neurospheres were able to differentiate by extending their axons, leading to the expression of specific axonal markers. Interestingly the direction of the axons was able to follow the one of the skeletal muscle fibers, suggesting again how the tension exerted by our PDMS support plays a crucial role in controlling the constructs morphology. Finally we observed an increased trend in the number of bungarotoxin clusters, suggesting the generation of bona fide in vitro neuromuscular junctions (Figure 17).

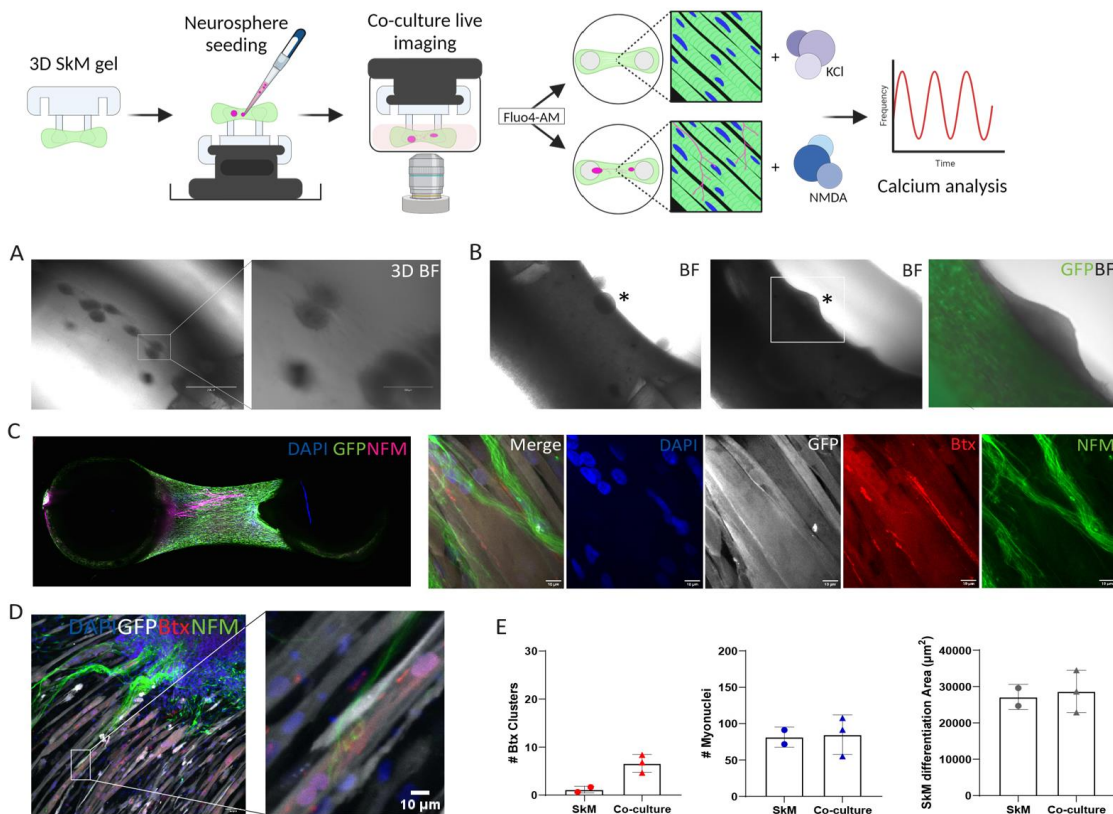


Figure 17 *In vitro* generation of 3D neuromuscular constructs adapting our PDMS supports.

To fully investigate the benefits of the co-culture, we tested the metabolic activity of our miniaturized 3D skeletal muscle with and without the neuronal component, by looking at the calcium transients. Preliminary data (Figure 18) support the idea that the addition of the neuronal component is able to support the generation of a more physiological environment, with a higher chance to observe spontaneous tissue twitching.

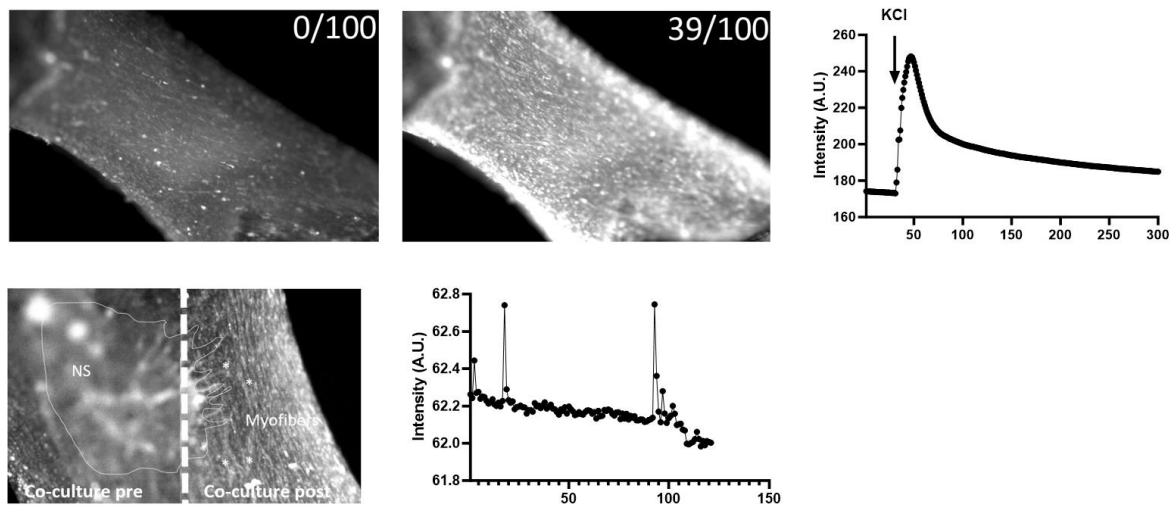


Figure 18 Calcium transients in 3D miniaturized skeletal muscle and 3D neuromuscular constructs.

## 2. Stimulation of miniaturized 3D muscle

During this phase of the project we have also optimised strategies for stimulating the engineered muscle construct, in both the platform generated by BIOND and KCL.

Regarding the MUSbit™ Chip, after initial confirmation of the formation of muscle microtissues in Deliverable 1.1, we functionally tested the microtissues using BIOND's internally developed stimulation tool compatible with MUSbit™ Chip. We based the initial parameters for stimulation (voltage, pulse-width, frequency, pulse train duration) on literature with similar devices. During stimulation, images were captured at a 10-fps framerate, after which we performed image-based analysis (MUSCLEMOTION) to calculate the contraction amplitude. We then performed voltage and pulse width sweeps to find the optimal parameters, which in our hands were 5V 10ms biphasic pulses.

To assess a force-frequency relationship, we stimulated WT muscle microtissues with biphasic pulses (5V, 10ms pulse width, 1s pulse train) with increasing frequencies (Figure 19, A). Here we find that at low frequencies (<10 Hz) twitch contractions can be generated, with lower contraction amplitude than at higher frequencies (>10 Hz). While tetanic contractions could already be observed at 20 Hz with a 1s pulse train duration, we chose to use 30 Hz with a 3s pulse train duration as a Tetanic stimulation for all future experiments, to make sure the whole bundle was contracted. For Twitch we used a single pulse.

Using these Twitch and Tetanus parameters we measured the contraction of WT and DMD microtissues at Day 7, Day 10 and Day 14. In Figure 19, B, representative traces of Twitch (top) and tetanus (bottom) can be seen. First, we see that for all genotypes, tetanic stimulation generally showed higher peak contraction amplitudes than twitch stimulations (as expected). Secondly, we see that the peak contraction amplitude was generally higher for WT than for either DMD $\Delta$ 44 or DMD $\Delta$ 52 with both twitch and tetanic stimulations. This difference is even more pronounced in the sustained contraction stimulation, in which we keep stimulating the tissue with 30 Hz pulses for a duration of 10s (Figure 19, C). In general, for WT tissues, an increase in peak contraction amplitudes was seen with increased culture time. In contrast, dystrophic tissues show similar peak contraction amplitudes across all measured timepoints. This could possibly indicate a difference in maturation, although further characterization will need to be performed to confirm this. Together these data highlight that we have established a functional assay with electrical stimulation, and that with our model system we are able to differentiate functional differences between WT and dystrophic tissues.

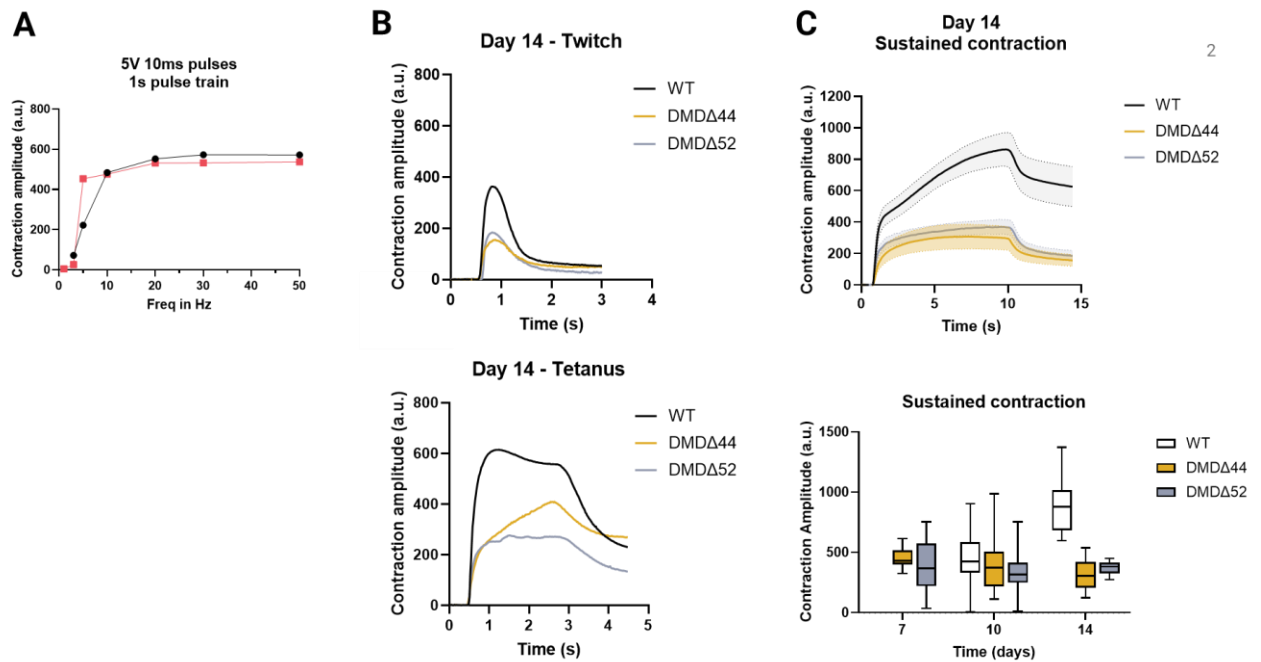


Figure 19 Electrical stimulation and measurement of contraction for WT and DMD iPSC-based muscle microtissues. (A) Measurement of contraction with increasing pulse frequency. (B) Representative traces of WT and DMD microtissues stimulated with twitch or tetanic pulses at Day 14. (C) Average contraction amplitude  $\pm$  95% CI of sustained contraction at Day 14 (top), and boxplots of peak contraction amplitudes at Day 7, 10 and 14 (bottom).

Having demonstrated functionality and disease phenotyping through our electrical stimulation of miniaturized 3D muscles, we next proceeded to mechanical stimulation of skeletal muscle using KCL develop platform. We considered the possibility to mimic the muscle contraction in vitro by engineering our miniaturized PDMS support, for different purposes as the idea of recreating in vitro the physiological and pathological modes of skeletal muscles elongation. To achieve this goal, we have conceived an innovative platform (Figure 20) based on the combined use of a magnetic bar, added in one of the feet of the PDMS support, and an electromagnet. Thanks to the activation of the electromagnet, we can control the displacement of the magnetic PDMS pillar, effectively mimicking the skeletal muscle mechanics.

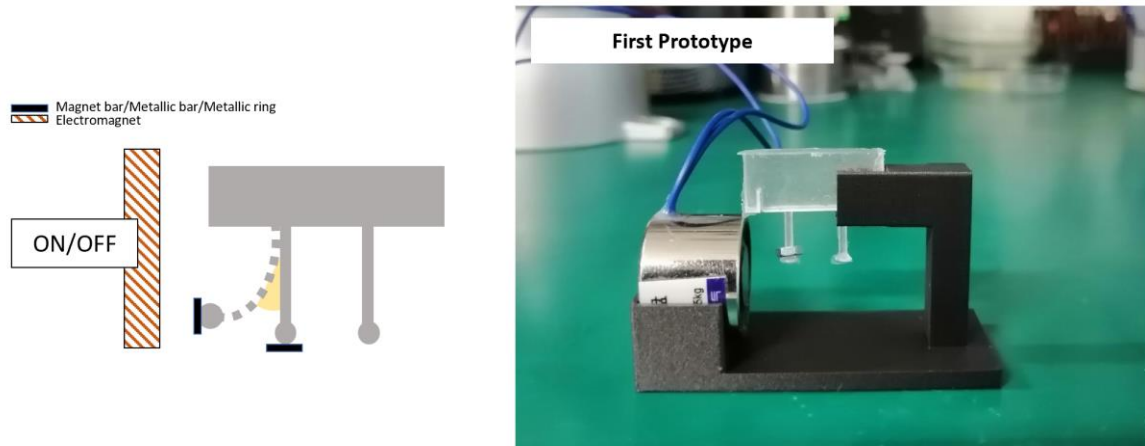


Figure 20 The prototype of the electromagnet platform.

From the prototype, we then decided to design and fabricated a more complex electromagnet platform, a compact 3D printed structure (<20 cm), equipped with culture chambers and a live camera, for being able to cultivate our miniaturized 3D constructs in the standard incubator while observing the tissue mechanical stimulation (Figure 21).

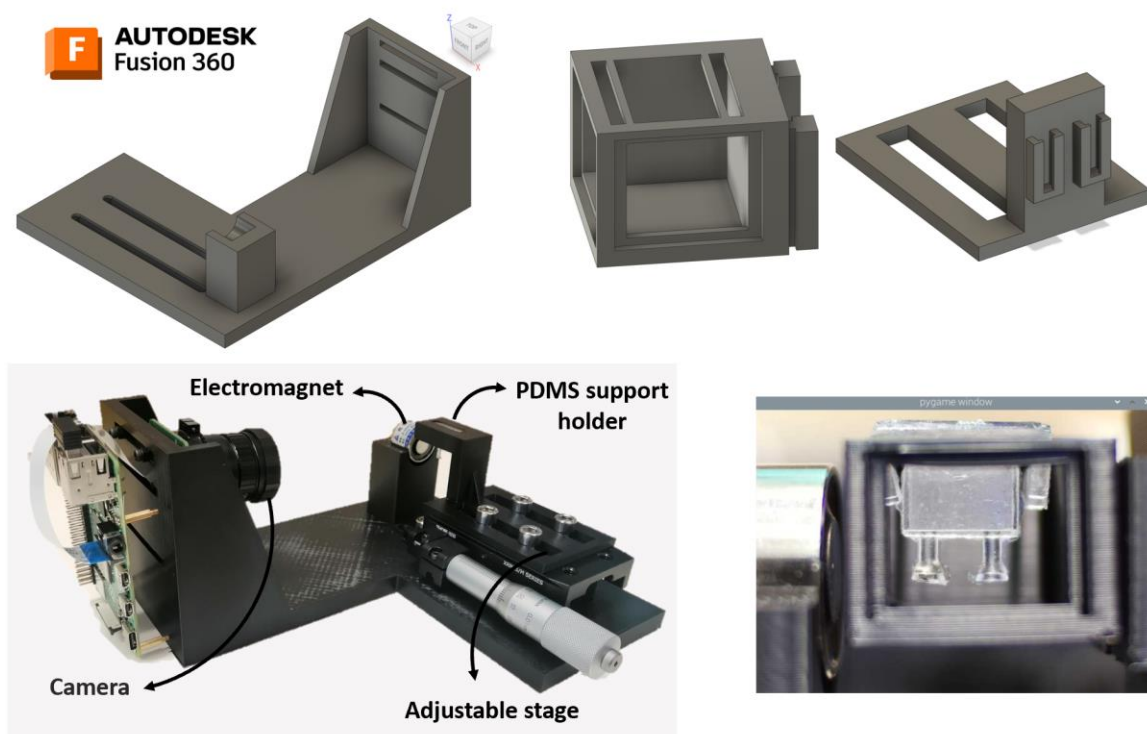


Figure 21 The electromagnet platform, with all its components.

Moreover, by controlling and reverting the polarity of the PDMS embedded magnetic bar, we were able to mimic in vitro not only the skeletal muscle elongation, but also its contraction (Figure 22).

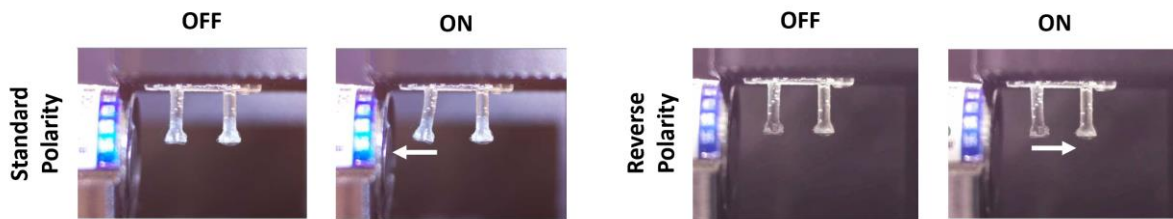


Figure 22 Elongation and contraction of the magnetic pillar using standard and reverse polarity.

### 3. Perfusion of our 3D muscle generation devices

Finally, we proved the versatility of our PDMS based miniature muscle forming pipeline by generating perfusable PDMS supports. To our knowledge, the possibility to deliver in a controlled and precise fashion chemicals as well as AAV vectors, plays a key role in mimicking in vitro the in vivo skeletal muscle vascular flow. To achieve this goal, we adapted our negative mould design for the generation of straight or bended channels (Figure 23).

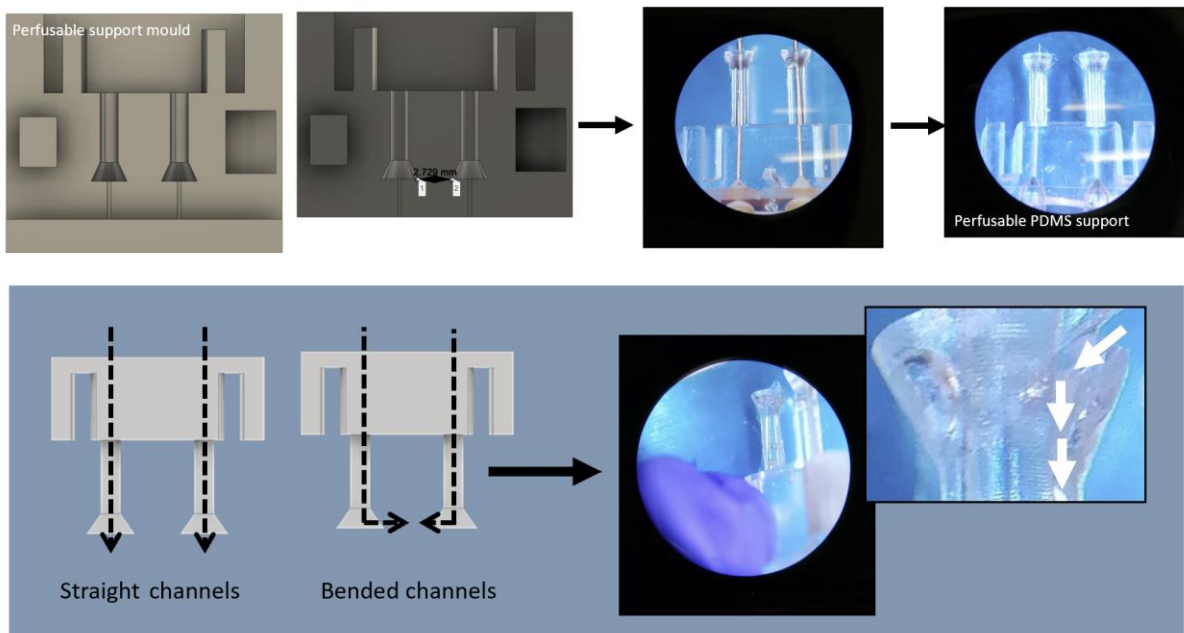


Figure 23 Straight channel negative mould design and respective PDMS support.

We then tested our perfusable PDMS supports with the 3D skeletal muscle gels. As proof of principle, we checked if the presence of the straight channels was compatible with skeletal muscle differentiation, we observed not only the ability of myoblasts to fuse and form myofibers, but also the tissue contraction after KCl administration directly in the PDMS channels (Figure 24). Overall, we can conclude that our pipeline can be adjusted to generate functional miniaturized PDMS supports suitable for the perfusion of 3D in vitro skeletal muscle.

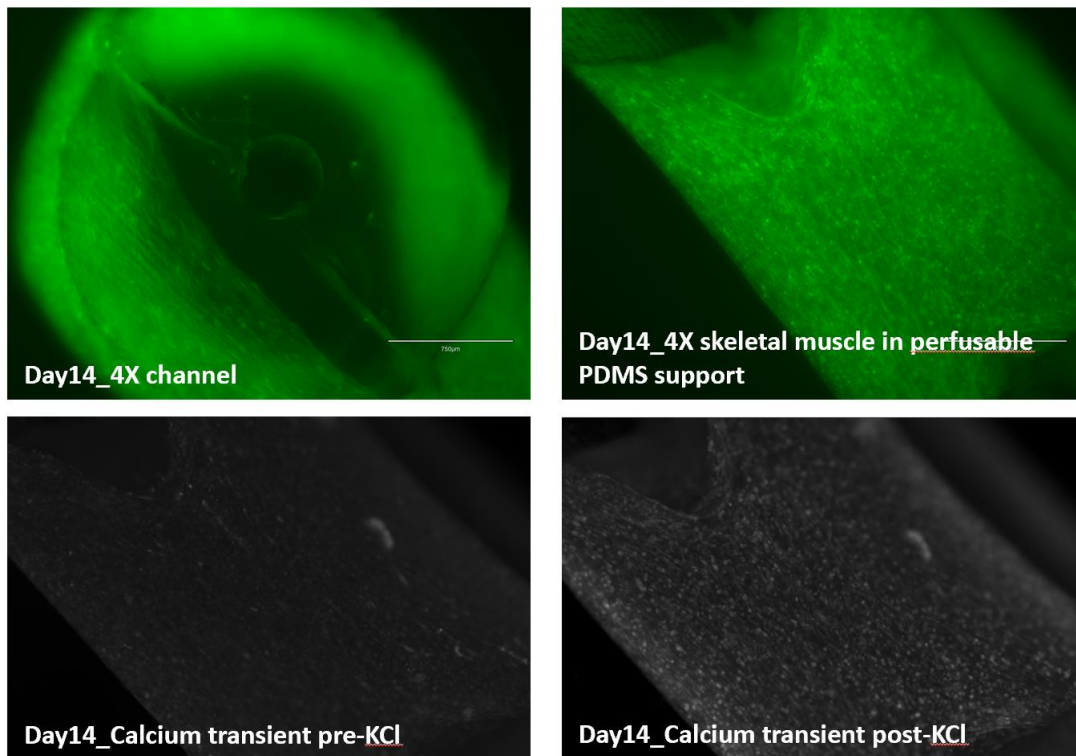


Figure 24 3D skeletal muscle differentiation in straight channel PDMS support with respective calcium transients.

In our second approach with **comPLATE™** with **Pneumatic device**, we designed the perfusion channel to be adjacent to 3D muscles. We conducted three main activities to validate the perfusion capabilities of this system. First, we calibrated the system to determine how the concentration of a compound can be controlled within the microfluidic system. Next, we investigated the impact of flow on both the morphology and function of the tissue. Finally, we introduced a compound into the system through the microfluidic component and studied how the contraction forces of the tissues were dynamically affected by it.

- i. **Calibration:** A fluorescent dye was used to measure the behavior of flow within the organ-on-chip system. The setup, shown in Figure 25, involves the **comPLATE™** interface with the **MUSbit™** chip. In this configuration, a fluorescent dye of known concentration is introduced or flushed out to observe diffusion and perfusion characteristics over time.

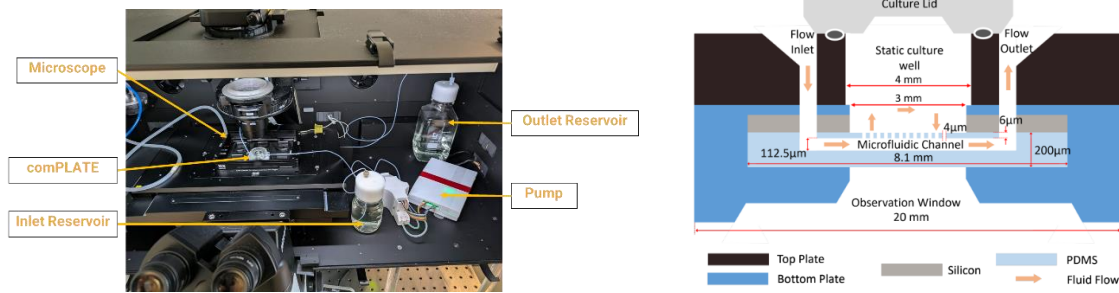


Figure 25 Left - Microscope setup with the comPLATE; Right - comPLATE™ cross section with MUSbit™

Dextran dye [FITC-Dextran FD40S-100MG], a widely-used fluorescent tracer, was chosen for its stability, pH insensitivity to solvents, and predictable fluorescence at specific excitation and emission wavelengths of 405nm. Different flow rates were analysed to understand how concentration and intensity values correlate with running in and flushing out the dye from the comPLATE, allowing us to assess parameters such as diffusion rates, optimal concentration ranges, and impacts of dilution on fluorescence intensity.

For the run-in experiments (left in Figure 26), the well is filled with 200μl of PBS (blue) and the dye (green) is pumped at a certain flow rate for a known period of time. For the flush-out experiments (right in Figure 26), the well is filled with 200μl of the dye (green) which is flushed out with PBS at a set flow rate certain period of time. In all cases the concentration of the dye and its corresponding fluorescent intensity were recorded. The tubing length for the pneumatic device were measured and kept constant throughout the measurement.

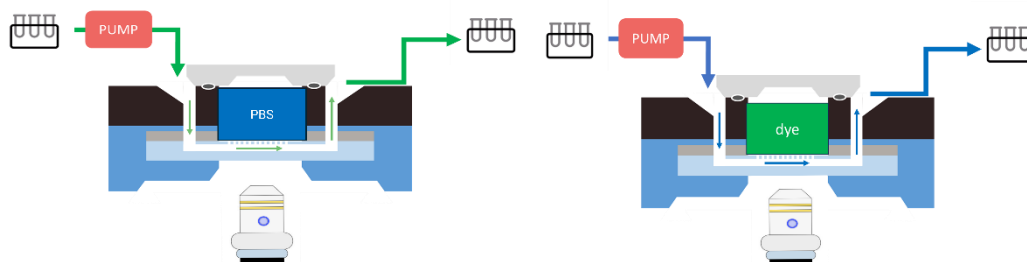


Figure 26 Left – Run-in Setup; Right – Flush-out Setup

To characterize the dye quantification results for the perfusion system, a stock solution of 0.125 mg/mL was prepared using a buffered PBS solution as the solvent. The advantage of using PBS over water is that it minimizes or eliminates pH changes within the buffered solution. The total volume of the comPLATE™ is considered to be 200 μL, meaning that 200 μL of dye corresponds to 100% dye concentration in the well. Specific measurements were taken to ensure the microscope could detect intensity up to this volume within the comPLATE™. The graph (Figure 27) shows a linear increase in intensity as the volume of fluorescent dye was increased in the well of the comPLATE™.

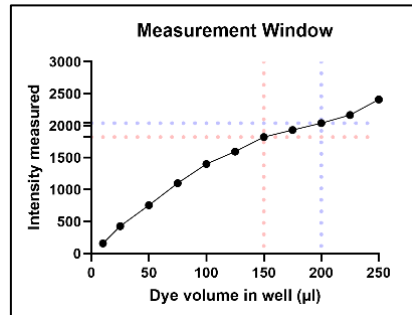


Figure 27 Measuring the detectable volume within the setup

The behaviour is linear up to 150µl, after which the linearity of the graph is affected slightly. This could be because the resolution of the fluorescence measured in the well starts to reduce when the dye volume is over 150µl (the orange line) worth of height in the comPLATE™ and perhaps the errors post 200µl (the purple line) become more evident as the difference reduces.

To correlate intensity measured to the concentration of the dye in the well, different solutions are derived from this stock. The Figure 28 shows the calibration graph hence obtained.

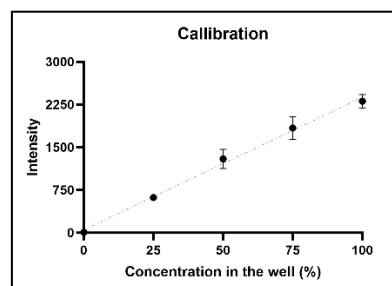


Figure 28 Calibration Curve for different concentration of dye in the well (NOTE- concentration measured over a volume of 200µl)

The linear line gives the required equation  $[y = 2195.5 \cdot x; \text{ where } y \text{ is the measured intensity and } x \text{ is the concentration in the well}]$  used while analysing the concentration change during various run in and flush out experiments.

To ensure the intensity measured in the well is not affected by the amount of PBS present in the well, dilution test were done. The well is filled with a known volume of dye, and the intensity is measured. The well is then further diluted with PBS in steps and the intensity of the new volume present in the well is measured. In every case, the plate is centrifuged to make sure the contents in the well are mixed well. We observed that the the measured value of fluorescence is the only related to volume of the dye in the well, with increasing volumes of PBS filling the well had a minimal effect on reducing the intensity value.

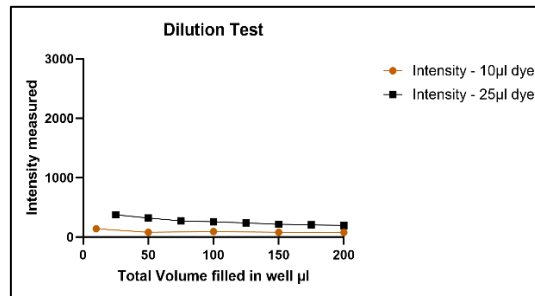


Figure 29 Dilution tests

To measure the sensitivity of the setup serial dilutions of the stock volume (molar mass – 0.125mg/ml, shown as the black dotted line in Figure 29) was implemented from 1:1 to 1:24 parts. The dilution was done in PBS. The graph (Figure 30) shows the relation between the absolute concentration, molar mass (in mg/ml) and intensity. The smallest value that was able to be measured was 1:24 diluted dye solution which is 0.00625mg/ml (or 6.25 $\mu\text{g/ml}$ ).

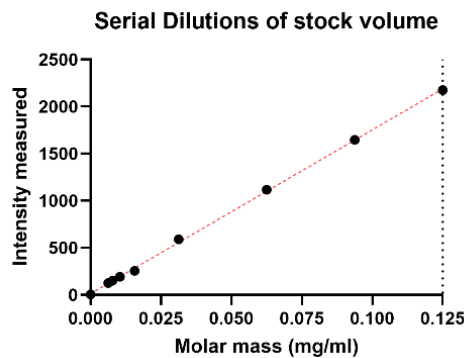


Figure 30 Measured intensity at different molar masses of the dye

[NOTE - volume considered for measurement - 200 $\mu\text{l}$ ]

Based on the condition for run-in or flush-out (explained in Figure 26), the microscope settings (exposure time and capture rate) are kept the same. The change in intensity of fluorescence is then obtained throughout the experiment which is then correlated to achieve the graphs of how the concentration of the dye

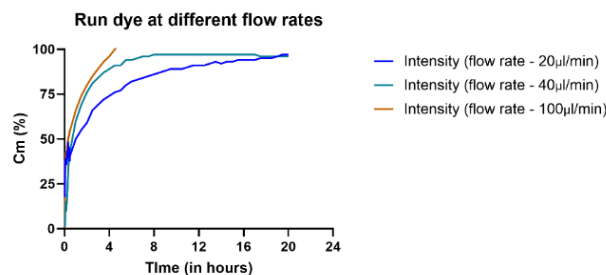


Figure 31 Run in dye Summary [Cm- measured concentration]

behaves inside the comPLATE™ setup. The volume of medium (PBS – run-in and Dye – flush-out) is 200µl in the well, at the start of the experiment.

It was observed that if  $x$  concentration of the dye is perfused in the comPLATE™, at different flow rates, the final concentration that reached the well was  $x$ . The speed at which this happens is directly dependent on the flow rate (high flow speeds, for instance at 100µl/min, meaning faster saturation of the dye in the well compared to a flow rate of 20µl/min).

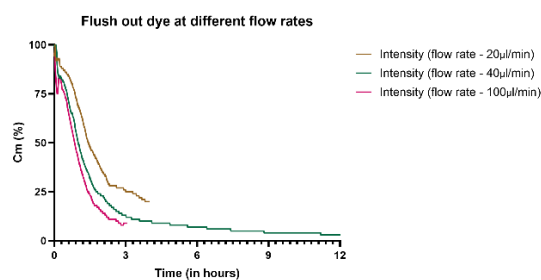
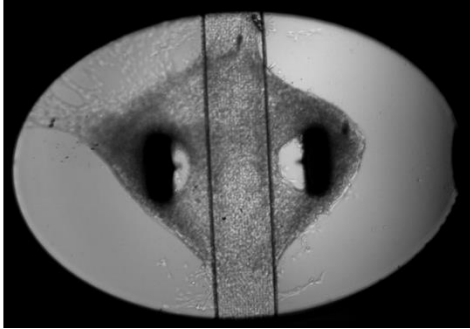


Figure 32 Flush out Dye summary [ Cm – measured Concentration]

Similarly it was seen with flush out experiments that majority of the dye can be flushed out within the perfusion setup. There could be regions in the well (regions away from the pores on the channel) which might be difficult to be flushed. In drug based application, multiple flushing cycles could be implemented to effectively have no dye present in the well.

- ii. Muscle tissue under 24 hours of constant flow:** Next we wanted to apply flow to our muscle tissue model. To this end, we first optimized the seeding conditions for tissue formation in our MUSbit™ chip, containing the microfluidic channel underneath the pillar system, separated by a porous membrane. We found that with our normal seeding protocol, the cell/gel mixture tended to flow into the microfluidic channel, leading to distorted microtissues (Figure 33, A).

**A**



**B**

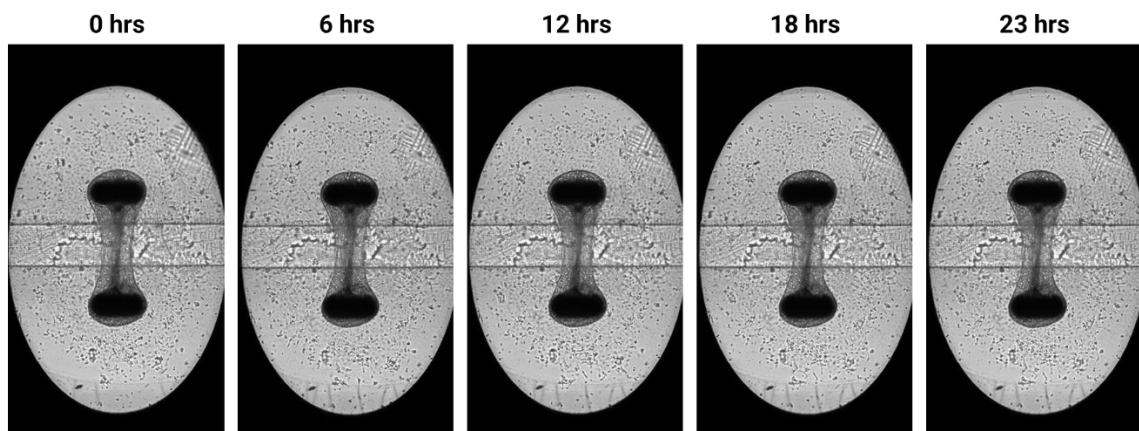


Figure 33 (A,B) C2C12 muscle microtissue under a constant 30 µl/min flowrate for 23 hours

After several troubleshooting steps, we managed to generate microtissues in our MUSbit™ / comPLATE™ platform. We then used the internally-developed pneumatic device to apply flow to the microtissues. First, we started with low flow rates (5 µl/min), but gradually increased the flow rate to 30 µl/min. At this flow rate we find that the tissue did not detach, nor change its morphology, even for a duration of at least 23 hours of dynamic flow (figure 33, B).

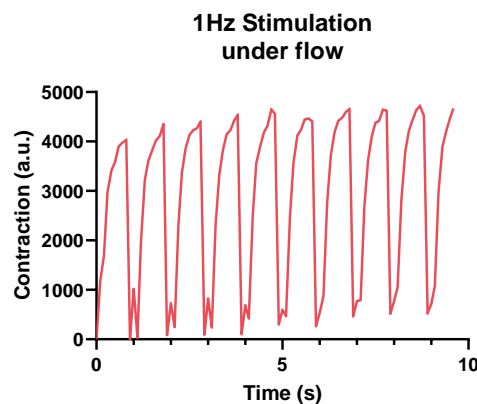


Figure 34 Muscle contraction under simultaneous 1 Hz electrical pacing and 30 µl/min perfusion

